I. Troch, F. Breitenecker, eds. ISBN 978-3-901608-35-3

Influence of Detector Bandwidth and Detector Size to the Resolution of Photoacoustic Tomography

Markus Haltmeier[1], Otmar Scherzer[1,2], Gerhard Zangerl[1]
[1]Department of Mathematics, University of Innsbruck, Austria,
[2]Radon Institute of Computational and Applied Mathematics, Linz, Austria

Corresponding author: Markus Haltmeier, University of Innsbruck, Department of Mathematics, 6020 Innsbruck, Technikerstraße 21a, Austria, markus.haltmeier@uibk.ac.at

Abstract. High spatial resolution is one of the major aims in photoacoustic tomography. Two main factors limiting the resolution of photoacoustic tomography are the detector size and the finite bandwidth of the ultrasound detection system. We present a quantitative analysis of those effects for "approximate point detectors" and for "approximate line detectors".

Keywords. Photoacoustic tomography; image reconstruction; wave equation; resolution; bandwidth.

AMS classifications. 44A12, 65R32, 35L05, 92C55.

1 Introduction

Photoacoustic tomography (PAT) is a novel imaging method for visualizing the electromagnetic absorption coefficient of a medium at low frequencies. It is based on the excitation of high bandwidth acoustic waves by illuminating a probe with pulsed electromagnetic energy, and combines the advantages of optical (high contrast) and ultrasonic imaging. We refer the reader to [22, Section 1.5] for a detailed mathematical description. PAT has proven great promise for a variety of biomedical applications, such as imaging of animals [15, 23], early cancer diagnostics [16, 19], and imaging of vasculature [4, 14]

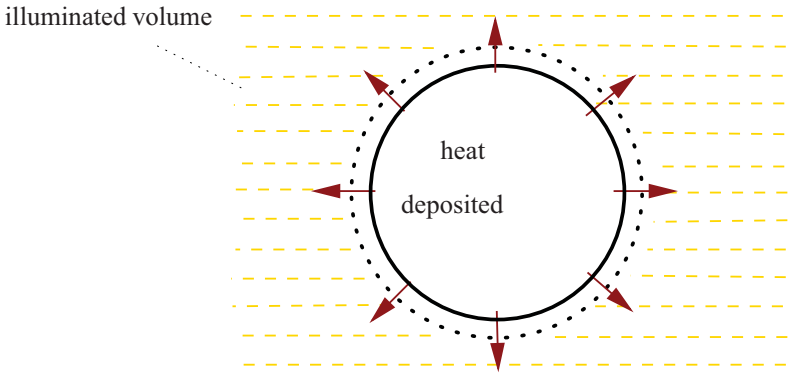

Figure 1: Thermoelastic effect: Parts of a specimen are illuminated with electromagnetic energy and react with expansion

If a probe is illuminated with a short pulse of non-ionizing electromagnetic radiation, it absorbs a fraction of energy, heats up, and reacts with an expansion (the so called thermoelastic effect; see figure 1). This in turn induces an acoustic wave, which is recorded outside of the object. Other than in conventional ultrasound imaging, where the source of the acoustic wave is an external transducer, in PAT the source is the imaged object itself. The frequency bandwidth of the recorded signals is therefore generally broad and depends on the size and the shape of illuminated structures.

If we assume that the probe is acoustically homogeneous, then the excited acoustic pressure $p : \mathbb{R}^3 \times (0,\infty) \to \mathbb{R}$ satisfies

$$\left(\partial_t^2 - \Delta\right) p(\mathbf{x},t) = 0\,, \qquad (\mathbf{x},t) \in \mathbb{R}^3 \times (0,\infty)\,, \tag{1a}$$

$$p(\mathbf{x},0) = f(\mathbf{x})\,, \partial_t p(\mathbf{x},0) = 0\,, \qquad \mathbf{x} \in \mathbb{R}^3\,, \tag{1b}$$

where Δ denotes the Laplacian with respect to the spatial variable $\mathbf{x}$ and ∂_t is the derivative with respect to the temporal variable t. For simplicity of presentation we assume throughout that $f \in C_c^\infty(B_R)$, where $B_R \subset \mathbb{R}^3$ is the ball with radius R centered at the origin. Here and in the following, $C_c^\infty(\Omega)$ denotes the space of all smooth functions $f : \mathbb{R}^3 \to \mathbb{R}$ with have compact support in the set $\Omega \subset \mathbb{R}^3$.

In the following we denote by $\mathscr{W}^{3D} : C_c^\infty(\mathbb{R}^3) \to C^\infty(\mathbb{R}^3 \times (0,\infty))$ the operator that takes smooth compactly supported initial data to the solution of (1a), (1b). The goal of PAT is to reconstruct the initial pressure f (representing the probe) from measurements of $(\mathscr{W}^{3D} f)(\mathbf{x},t)$ taken outside of B_R.

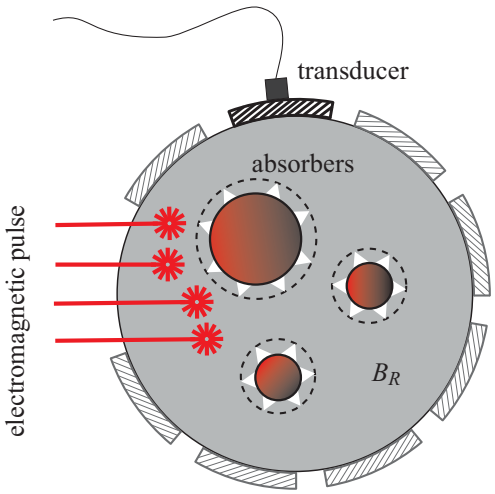

Figure 2: Photoacoustic tomography with piezoelectric transducer as an "approximate point detector".

1.1 Approximate point-detectors

The classical approach in PAT is to assume that point data

$$(\mathbf{P}f)(\mathbf{z},t) := g(\mathbf{z},t) := (\mathscr{W}^{3D}f)(\mathbf{z},t)\,, \qquad (\mathbf{z},t) \in \partial B_R \times (0,\infty)\,,$$

are given (∂B_R denotes the boundary of B_R). The operator $\mathbf{P} : C_c^\infty(B_R) \to C^\infty(\partial B_R \times (0,\infty))$ that maps a compactly supported initial data to the data measured by an ideal point detector can be inverted uniquely [1, 2]. In [6, 7] it is shown that $\mathbf{P}$ is an isometry with respect to the inner products $\int_{B_r} f_1 f_2$ and $2/R \int_{\partial B_R \times (0,\infty)} t g_1 g_2$ on $C_c^\infty(B_R)$ and $C^\infty(\partial B_R \times (0,\infty))$, respectively. The inversion is therefore even stable with respect to the L^2 topologies. Exact expressions for its inverse

$$\mathbf{P}^{-1} : \mathrm{ran}(\mathbf{P}) \subset C^\infty(\partial B_R \times (0,\infty)) \to C_c^\infty(B_R)$$

are derived in [6, 17, 25]. Here and in the following $\mathrm{ran}(\mathbf{P}) := \{\mathbf{P}f : f \in C_c^\infty(B_R)\}$ denotes the range of $\mathbf{P}$.

In practical applications, the detection system has a finite bandwidth. Moreover, standard ultrasound transducers, which integrate the pressure over its surface, are used to approximate point data. If we assume that the transducer surface is part of the measurement surface and rotationally symmetric (see Fig. 2), then the measured data are given by

$$(\mathbf{P}_{\phi,w}f)(\mathbf{z},t) = \left[\phi *_t \int_{\partial B_R} w\left(|\mathbf{z}-\mathbf{z}'|\right)(\mathscr{W}^{3D}f)(\mathbf{z}',\cdot)\,dS(\mathbf{z}')\right](t)\,, \qquad (\mathbf{z},t) \in \partial B_R \times (0,\infty)\,.$$

Here $w(r)$ represents the sensitivity of the detector surface, $\phi(t)$ denotes the impulse response function of the ultrasound detection system, and $*_t$ is the convolution with respect to t.

Insufficient knowledge of w and ϕ, as well as the severe ill-posedness of deblurring problems make it impossible to stably invert $\mathbf{P}_{\phi,w}$. It is therefore common to apply the exact inverse of $\mathbf{P}$ to the data $\mathbf{P}_{\phi,w}f$. This results in a blurred reconstruction, where the blurring depends, e.g., on the detector size. Exact blurring kernels will be given in Subsection 1.3.

1.2 Approximate line-detectors

In order to partly overcome the size and shape limitations of point detectors, in [3, 11, 21] we propose PAT with line integrals

$$(\mathbf{L}f)(\mathbf{z},t) := \int_{\ell_\mathbf{z}} (\mathscr{W}^{3D}f)(\mathbf{x},t)\,dS(\mathbf{x})\,, \qquad (\mathbf{z},t) \in \partial B_R \times (0,\infty)\,,$$

where $\ell_\mathbf{z}$ is the unique line passing through $\mathbf{z}$, being tangential to ∂B_R, and orthogonal to $\mathbf{e}_3$. The inversion of $\mathbf{L}$ requires a two step reconstruction procedure:

- For fixed orientation of $\ell_\mathbf{z}$, the data $(\mathbf{L}f)(\mathbf{z},t)$ is the solution of the two dimensional wave equation where the initial data are given by the linear projection of f in that direction [11]. Hence linear projections of f can be obtained by recovered the initial data of the two dimensional wave equation from values of its solution on a circle.
- In a second stage, a three dimensional image is reconstructed from the projection images by applying the inverse two dimensional classical Radon transform in planes orthogonal to the rotation axis.

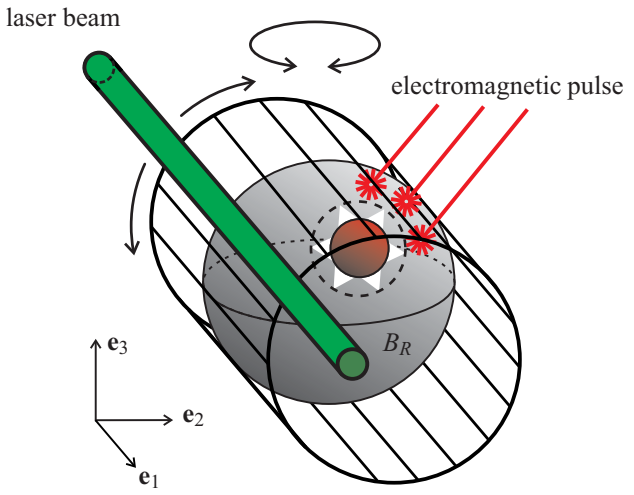

Figure 3: Photoacoustic tomography with a laser beam as "approximate line detector".

The operator $\mathbf{L} : C_c^\infty(B_R) \to C^\infty(\partial B_R \times (0,\infty))$ that maps a compactly supported initial data to the data measured by an ideal line detector can be inverted uniquely. Exact inversion formulas have been derived in [5, 11, 17, 18].

In practical applications the line detector is approximated by a cylindrically symmetric laser beam that is part of an interferometric setup (see Fig. 3). Such a laser naturally integrates the pressure over its volume [9, 21], and thus

$$(\mathbf{L}_{\phi,w} f)(\mathbf{z},t) = \left[\phi *_t \int_{\mathbb{R}^3} w\big(\operatorname{dist}(\ell_{\mathbf{z}},\mathbf{x})\big) (\mathscr{W}^{3D} f)(\mathbf{x},t) d\mathbf{x} \right], \qquad (\mathbf{z},t) \in \partial B_R \times (0,\infty)$$

are the actually available data. Here $w(r)$ represents the radial profile of the detecting laser beam, $\phi(t)$ is the impulse response function of the ultrasound detection system, and $\operatorname{dist}(\ell_{\mathbf{z}},\mathbf{x})$ denotes the distance between line $\ell_{\mathbf{z}}$ and point $\mathbf{x}$.

Again, application of $\mathbf{L}^{-1} : \operatorname{ran}(\mathbf{L}) \to C_c^\infty(B_R)$ to the data $\mathbf{L}_{\phi,w} f$ leads to a blurred reconstruction. However, the laser beam can be made very thin, suggesting that the one dimension approximation with approximate line detectors gives less blurred images than the zero dimension approximation with approximate point detectors. Our aim is to make such statements precise, by calculating analytical blurring kernels and to investigate the resolution for both kind of detectors.

1.3 Analytic expressions for blurring kernels

Our first result explicitly characterizes the blurring kernel of point detectors:

Theorem 1. *Let $f \in C_c^\infty(B_R)$, and let $\phi, w : \mathbb{R} \to \mathbb{R}$ be even function such that $\mathbf{x} \in \mathbb{R}^3 \mapsto \phi'(|\mathbf{x}|)/|\mathbf{x}|$ and $\mathbf{z} \in \partial B_R \mapsto w(|\mathbf{z}-\mathbf{z}_0|)$, are absolutely integrable, for some $\mathbf{z}_0 \in \partial B_R$. Moreover, assume that $\operatorname{supp}(\phi) \subset [-\tau,\tau]$, where $\tau := \operatorname{dist}\big(\operatorname{supp}(f), \partial B_R\big)$ and $\operatorname{supp}(\phi) := \overline{\{t : \phi(t) \neq 0\}}$.*

Then $\mathbf{P}_{\phi,w} f \in \operatorname{ran}(\mathbf{P})$ and

$$\big(\mathbf{P}^{-1} \mathbf{P}_{\phi,w} f\big)(\mathbf{x}) = \left[\Phi_{\text{band}} * \int_{\mathbb{R}^3} W_{\text{point}}(\cdot,\mathbf{x}') f(\mathbf{x}')\, d\mathbf{x}' \right](\mathbf{x}), \qquad \mathbf{x} \in B_R, \tag{2}$$

with the blurring kernels

$$\Phi_{\text{band}}(\mathbf{x}) := -\pi \phi'(|\mathbf{x}|)/(2|\mathbf{x}|), \qquad \mathbf{x} \in \mathbb{R}^3, \tag{3}$$

$$W_{\text{point}}(\mathbf{x},\mathbf{x}') := \frac{R^2}{|\mathbf{x}|^2} \delta\big(|\mathbf{x}| - |\mathbf{x}'|\big)\, w\big(|\mathbf{x}-\mathbf{x}'|\, R/|\mathbf{x}|\big), \qquad \mathbf{x},\mathbf{x}' \in \mathbb{R}^3. \tag{4}$$

Proof. See Section 2. □

As a consequence of Theorem 1, the detector aperture causes blurring in the lateral direction, which becomes more severe near to the recording surface. The finite bandwidth, on the other hand, causes spatially invariant blurring.

We will also prove a corresponding result for approximate line detectors:

Theorem 2. *Let $f \in C_c^\infty(B_R)$, and let $\phi, w : \mathbb{R} \to \mathbb{R}$ be even functions such that $\mathbf{x} \in \mathbb{R}^3 \mapsto \phi'(|\mathbf{x}|)/|\mathbf{x}|$ and $\mathbf{x} \in \mathbb{R}^3 \mapsto \int_{|\mathbf{x}|}^\infty \partial_\xi w(\xi)/\sqrt{\xi^2 - |\mathbf{x}|^2}\, d\xi$ are absolutely integrable. Moreover, assume that $\operatorname{supp}(\phi * w) \subset [-\tau,\tau]$, where $\tau := \operatorname{dist}\big(\operatorname{supp}(f), \partial B_R\big)$.*

Then $\mathbf{L}_{\phi,w} f \in \mathrm{ran}(\mathbf{L})$ *and*

$$\left(\mathbf{L}^{-1}\mathbf{L}_{\phi,w} f\right)(\mathbf{x}) = \left(\Phi_{\mathrm{band}} * W_{\mathrm{line}} * f\right)(\mathbf{x}), \qquad \mathbf{x} \in B_R, \tag{5}$$

where Φ_{band} *is as in (3), and*

$$W_{\mathrm{line}}(\mathbf{x}) := -\frac{1}{\pi}\int_{|\mathbf{x}|}^{\infty} \frac{\partial_\xi w(\xi)}{\sqrt{\xi^2 - |\mathbf{x}|^2}}\, d\xi, \qquad \mathbf{x} \in \mathbb{R}^3. \tag{6}$$

Here both blurring effects are spatially invariant.

Proof. See Section 3. □

1.4 Prior work and innovations

Analytic expressions for the blurring kernels with approximate line detectors are presented for the first time. Exact blurring kernels for approximate point detectors have also been derived in [24]. However, we present a completely different and probably simpler analysis, which is based on geometric arguments and the rotational invariance of the wave equation. Moreover, in [24] the authors did not show that $\mathbf{P}_{\phi,w} f \in \mathrm{ran}(\mathbf{P})$. Instead, they applied a particular inversion formula (i.e. an extension of $\mathbf{P}_{\mathrm{point}}^{-1}$ outside the range of $\mathbf{P}_{\mathrm{point}}$) to the blurred data. Hence their results depend on the used extension, whereas our results are independent of any particular inversion formula. On the other hand, the results of [24] can be applied even if ϕ is non-symmetric, in which case $\phi *_t (\mathbf{P}_{\mathrm{point}} f) \notin \mathrm{ran}(\mathbf{P})$.

2 Blurring kernels for approximate point detectors

The main goal in this section is the derivation analytic expressions for the blurring kernels due to the detector size and bandwidth. The proof of of Theorem 1 will follow from the following Propositions 2.1 and 2.2 and will be given at the end of this section.

Proposition 2.1. *Let* $f \in C_c^\infty(B_R)$*, let* $w : \mathbb{R} \to \mathbb{R}$ *be an even function such that* $\mathbf{z} \in \partial B_R \mapsto w(|\mathbf{z} - \mathbf{z}_0|)$ *is absolutely integrable for some* $\mathbf{z}_0 \in \partial B_R$*, and define*

$$f_w(\mathbf{x}) := \int_{\mathbb{R}^3} \left[\frac{R^2}{|\mathbf{x}|^2}\delta(|\mathbf{x}| - |\mathbf{x}'|) w\big(|\mathbf{x} - \mathbf{x}'|\, R/|\mathbf{x}|\big)\right] f(\mathbf{x}')\, d\mathbf{x}, \qquad \mathbf{x} \in B_R.$$

Then

$$(\mathbf{P} f_w)(\mathbf{z}, t) := \int_{S_R} w\big(|\mathbf{z} - \mathbf{z}'|\big)(\mathbf{P} f)(\mathbf{z}', t) dS(\mathbf{z}'), \qquad (\mathbf{z}, t) \in S_R \times (0, \infty). \tag{7}$$

Proof. Our first goal is to calculate an expression for f_w without the Dirac δ function. To that end, denote $\mathbf{x} = \rho\sigma$, $\mathbf{x}' = \rho'\sigma'$ with $\rho, \rho' \in (0, \infty)$ and $\sigma, \sigma' \in S^2$. Then

$$\begin{aligned} f_w(\mathbf{x}) &= R^2 \int_{S^2} \left(\int_0^\infty \delta(\rho - \rho') w\big(|\rho\sigma - \rho'\sigma'|\, R/\rho\big) f(\rho'\sigma')\, d\rho'\right) d\sigma' \\ &= R^2 \int_{S^2} w\big(|\sigma - \sigma'|\, R\big) f(\rho\sigma')\, d\sigma'. \end{aligned}$$

Now define

$$p_w(\rho\sigma, t) := R^2 \int_{S^2} w\big(|\sigma - \sigma'|\, R\big)(\mathscr{W}^{3D} f)(\rho\sigma', t)\, d\sigma'.$$

We will show that $p_w = \mathscr{W}^{3D} f_w$, which then implies (7), since

$$\int_{S_R} w(|R\sigma - \mathbf{z}'|) p(\mathbf{z}', t) dS(\mathbf{z}') = R^2 \int_{S^2} w(R\,|\sigma - \sigma'|) p(R\sigma', t) d\sigma' = (\mathbf{P} f_w)(R\sigma, t), \qquad (R\sigma, t) \in S_R \times (0, \infty).$$

To that end, let $Q[\theta, \phi] : \mathbb{R}^3 \to \mathbb{R}^3$ be a rotation with

$$Q[\theta, \phi]\mathbf{e}_3 = (\sin\theta\cos\phi, \sin\theta\sin\phi, \cos\theta), \qquad (\theta, \phi) \in (0, \pi) \times (0, 2\pi).$$

Introducing spherical coordinates around axis σ shows that

$$\begin{aligned} p_w(\rho\sigma, t) &= R^2 \int_0^\pi \int_0^{2\pi} w\big(|\sigma - Q[\theta, \phi]\sigma|\, R\big)(\mathscr{W}^{3D} f)(\rho Q[\theta, \phi]\sigma, t) \sin\theta\, d\theta\, d\phi \\ &= R^2 \int_0^\pi w\big(2R(1 - \cos\theta)\big) \sin\theta \int_0^{2\pi} (\mathscr{W}^{3D} f)\big(Q[\theta, \phi](\rho\sigma), t\big) d\theta\, d\phi. \end{aligned}$$

The rotational invariance of the wave equation implies that $(\rho\sigma,t) \mapsto (\mathscr{W}^{3D} f)\big(Q[\theta,\phi](\rho\sigma),t\big)$ is a solution of the wave equation and its linearity implies that so is $p_w(\rho\sigma,t)$. Since the initial conditions $p_w(\mathbf{x},0) = f_w(\mathbf{x})$ and $\partial_t p_w(\mathbf{x},0) = 0$ immediately follow from the definition of p_w this implies $p_w = \mathscr{W}^{3D} f_w$ and concludes the proof. □

The next proposition deals with the blurring to the finite bandwidth of the detection system.

Proposition 2.2. *Let $f \in C_c^\infty(\mathbb{R}^3)$ and let $\phi : \mathbb{R} \to \mathbb{R}$ be an even compactly supported function such that $\Phi_{\text{band}}(\mathbf{x}) := -\pi\phi'(|\mathbf{x}|)/(2|\mathbf{x}|)$ is absolutely integrable. Then $\mathscr{W}^{3D}(\Phi_{\text{band}} * f)(\mathbf{x},t) = (\phi *_t \mathscr{W}^{3D} f)(\mathbf{x},t)$, for $\mathbf{x}$ outside the support of $\Phi_{\text{band}} * f$.*

Proof. Let $\Psi(\mathbf{x}) = \psi(|x|)$ be a radially symmetric absolutely integrable function. Our aim is to find an analytic expression for $\mathscr{W}^{3D}(\Psi * f)$ in terms of the solution $\mathscr{W}^{3D} f$ of (1a), (1b) and the to adjust Ψ such that $\mathscr{W}^{3D}(\Psi * f) = \phi *_t \mathscr{W}^{3D} f$ outside the support of $\Psi * f$.

D' Alemberts formula for the solution of the three dimensional wave equation (see [13]) applied to initial data $\Psi * f$ reads

$$\mathscr{W}^{3D}(\Psi * f)(\mathbf{x},t) = \frac{1}{4\pi}\partial_t t \int_{S^2} \left(\int_{\mathbb{R}^3} f(\mathbf{x}')\psi(\big|\mathbf{x}+t\omega-\mathbf{x}'\big|)d\mathbf{x}' \right) dS(\omega)\,.$$

Substituting $\mathbf{x}' = \mathbf{x} + \rho\sigma$, with $\rho > 0$ and $\sigma \in S^2$, in the inner integral, and applying Fubini's Theorem leads to

$$\begin{aligned}\mathscr{W}^{3D}(\Psi * f)(\mathbf{x},t) &= \frac{1}{4\pi}\partial_t t \int_{S^2} \left(\int_{S^2}\int_0^\infty f(\mathbf{x}+\rho\sigma)\psi(|\rho\sigma - t\omega|)\rho^2 d\rho dS(\sigma) \right) dS(\omega) \\ &= \partial_t t \int_0^\infty \int_{S^2} f(\mathbf{x}+\rho\sigma) \left(\frac{1}{4\pi}\int_{S^2} \psi(|\rho\sigma - t\omega|)dS(\omega) \right) \rho^2 d\rho dS(\sigma)\end{aligned}$$

The inner integral in the last expression is the (spherical) mean of $\Psi(\mathbf{x}) = \psi(|x|)$ over a sphere with radius t centered at $\rho\sigma$. Denoting by I_ψ a primitive of $s \mapsto \psi(\sqrt{s})$, then [12, Lemma 5.1] assures that

$$\frac{1}{4\pi}\int_{S^2} \psi(|\rho\sigma - t\omega|)dS(\omega) = \frac{I_\psi\big((\rho+t)^2\big) - I_\psi\big((\rho-t)^2\big)}{4t\rho}\,,$$

provided $\rho, t > 0$. Consequently

$$\mathscr{W}^{3D}(\Psi * f)(\mathbf{x},t) = \frac{1}{4}\partial_t \int_0^\infty \big(I_\psi\big((\rho+t)^2\big) - I_\psi\big((\rho-t)^2\big)\big)\,\rho \int_{S^2} f(\mathbf{x}+\rho\sigma)dS(\sigma)\,d\rho\,.$$

Differentiating under the integral leads

$$\mathscr{W}^{3D}(\Psi * f)(\mathbf{x},t) = \frac{1}{2}\int_0^\infty (\rho - t)\psi(|\rho - t|) \left(\rho \int_{S^2} f(\mathbf{x}+\rho\sigma)dS(\sigma) \right) d\rho\,, \qquad \mathbf{x} \notin \operatorname{supp}(\Psi * f)\,. \tag{8}$$

On the other hand, again by D' Alemberts formula, we have

$$(\phi *_t \mathscr{W}^{3D} f)(\mathbf{x},t) = \frac{1}{4\pi}\int_0^\infty \phi'(t-\rho) \left(\rho \int_{S^2} f(\mathbf{x}+\rho\sigma)dS(\sigma) \right) d\rho\,. \tag{9}$$

Equations (8) and (9) coincide if $s\psi(|s|) = -\frac{\pi}{2}\phi'(s)$ for all $s \in \mathbb{R}$. Since ϕ is assumed to be an even function, this is the case if

$$\psi(s) = -\frac{\pi}{2}\frac{\phi'(s)}{s}\,, \qquad s \geq 0\,.$$

This concludes the proof by taking $\Psi = \Phi_{\text{line}}$. □

Proof of Theorem 1. *Propositions 2.1 and 2.2 imply that*

$$\begin{aligned}(\mathbf{P}_{\phi,w} f)(\mathbf{x},t) &= \left(\phi *_t \int_{S_R} w(\big|\mathbf{z}-\mathbf{z}'\big|)(\mathscr{W}^{3D} f)(\mathbf{z}',\cdot)dS(\mathbf{z}') \right)(t) \\ &= \big(\phi *_t (\mathscr{W}^{3D} f_w)(\mathbf{x},\cdot)\big)(t) = \big(\mathscr{W}^{3D}(\Phi_{\text{band}} * f_w)\big)(\mathbf{x},t)\,, \qquad \mathbf{x} \notin \operatorname{supp}(\Phi_{\text{band}} * f)\,.\end{aligned}$$

Together with support hypothesis on ϕ this shows that $\mathbf{P}_{\phi,w} f = \mathbf{P}(\Phi_{\text{band}} * f_w)$. Therefore $\mathbf{P}_{\phi,w} f \in \operatorname{ran}(\mathbf{P})$ and $\mathbf{P}^{-1}\mathbf{P}_{\phi,w} f = \Phi_{\text{band}} * f_w$ which concludes the proof.

3 Blurring kernels for approximate line detectors

The main goal in this section is the proof analytic expressions for the blurring kernels due to the detector size and bandwidth of Theorem 2. In the following let $\mathscr{W}^{2D} : C_c^\infty(\mathbb{R}^2) \to C_c^\infty(\mathbb{R}^2 \times (0,\infty))$ denote the operator that takes a compactly supported initial data to the solution of the two dimensional wave equation

$$\left(\partial_t^2 - \Delta\right) p(\mathbf{x},t) = 0\,, \qquad (\mathbf{x},t) \in \mathbb{R}^2 \times (0,\infty)\,, \tag{10a}$$

$$p(\mathbf{x},0) = f(\mathbf{x})\,, \partial_t p(\mathbf{x},0) = 0\,, \qquad \mathbf{x} \in \mathbb{R}^2\,. \tag{10b}$$

First we calculate the blurring kernel due to the detector size. To that end, we will make use of the following Lemma:

Lemma 3.1 (Acoustic reciprocal principle in two dimensions)**.** *Let $f \in C_c^\infty(\mathbb{R}^2)$ and let Ψ be a compactly supported absolutely integrable function. Then $\Psi * (\mathscr{W}^{2D} f) = \mathscr{W}^{2D}(\Psi * f)$.*

Proof. D'Alemberts formula for the solution of (10a), (10b) is $(\mathscr{W}^{2D} f)(\mathbf{x},t) = \partial_t (g * f)(\mathbf{x},t)$ with

$$g(\mathbf{x},t) := \begin{cases} 1/\left(2\pi\sqrt{t^2 - |\mathbf{x}|^2}\right), & \text{if } t > |\mathbf{x}|\,, \\ 0\,, & \text{otherwise}, \end{cases}$$

see [13]. The symmetry of the convolution implies that

$$\Psi * (\mathscr{W}^{2D} f) = \Psi * \partial_t (g * f) = \partial_t (\Psi * g * f) = g * \partial_t (\Psi * f) = \mathscr{W}^{2D}(\Psi * f)\,,$$

and concludes the proof. □

Proposition 3.2. *Let $f \in C_c^\infty(\mathbb{R}^3)$, let $w : \mathbb{R} \to \mathbb{R}$ be a compactly supported even function such that $W_{\text{line}}(\mathbf{x}) = -1/\pi \int_{|\mathbf{x}|}^\infty \partial_\xi w(\xi)/\sqrt{\xi^2 - |\mathbf{x}|^2}\, d\xi$ is absolutely integrable.*

Then, for any line $\ell \subset \mathbb{R}^3$,

$$\int_{\mathbb{R}^3} w\big(\operatorname{dist}(\ell,\mathbf{x})\big)(\mathscr{W}^{3D} f)(\mathbf{x},t) d\mathbf{x} = \int_\ell \mathscr{W}^{3D}(W_{\text{line}} * f)(\mathbf{x},t) dS(\mathbf{x})\,. \tag{11}$$

Proof. Without loss of restriction we shall assume that ℓ is of the form $\ell = \mathbb{R}(1,0,0) + (0,z_1,z_2)$. Moreover we write $\mathbf{x} = (x_1,\mathbf{x}_2)$ with $x_1 \in \mathbb{R}$ and $\mathbf{x}_2$ in $\mathbb{R}^2$ and denote by $\mathbf{X}$ the X-ray transform restricted to lines pointing in $(1,0,0)$ direction,

$$(\mathbf{X}h)(\mathbf{x}_2) := \int_{\mathbb{R}} h(x_1,\mathbf{x}_2) dx_1\,, \qquad h \in C_c^\infty(\mathbb{R}^3)\,.$$

The commutation relation of the Laplacian with the X-ray transform implies that $\mathscr{W}^{2D}\mathbf{X} = \mathbf{X}\mathscr{W}^{3D}$, see [10, Theorem 1]. Therefore

$$\begin{aligned} \int_{\mathbb{R}^3} w(\operatorname{dist}(\ell,\mathbf{x})(\mathscr{W}^{3D} f)(\mathbf{x},t) d\mathbf{x} &= \int_{\mathbb{R}^2}\int_{\mathbb{R}} w(|\mathbf{z}_2 - \mathbf{x}_2|)(\mathscr{W}^{3D} f)((x_1,\mathbf{x}_2),t) dx_1 d\mathbf{x}_2 \\ &= \int_{\mathbb{R}^2} w(|\mathbf{z}_2 - \mathbf{x}_2|)(\mathbf{X}\mathscr{W}^{3D} f)(\mathbf{x}_2,t) d\mathbf{x}_2 \\ &= \big(w(|\cdot|) * (\mathbf{X}\mathscr{W}^{3D} f)\big)(\mathbf{z}_2,t) = \big(w(|\cdot|) * (\mathscr{W}^{2D}\mathbf{X} f)\big)(\mathbf{z}_2,t)\,. \end{aligned} \tag{12}$$

Let $U(\mathbf{x}) = u(|\mathbf{x}|)$ be a radially symmetric integrable function. Writing $\mathbf{x}' = (x_1',\mathbf{x}_2')$ with $x_1' \in \mathbb{R}$ and $\mathbf{x}_2'$ in $\mathbb{R}^2$, and applying Fubini's theorem shows

$$\begin{aligned} \mathbf{X}(U * f)(\mathbf{z},t) &= \int_\ell (U * f)(\mathbf{x},t) dS(\mathbf{x}) \\ &= \int_{\mathbb{R}} \left(\int_{\mathbb{R}}\int_{\mathbb{R}^2} u\big(((x_1 - \mathbf{x}_1)^2 + |\mathbf{x}_2 - \mathbf{x}_2'|^2)^{1/2}\big) f(x_1',\mathbf{x}_2') d\mathbf{x}_2' dx_1' \right) dx_1 \\ &= \int_{\mathbb{R}}\int_{\mathbb{R}^2} \left(\int_{\mathbb{R}} u\big(((x_1 - \mathbf{x}_1)^2 + |\mathbf{x}_2 - \mathbf{x}_2'|^2)^{1/2}\big) dx_1 \right) f(x_1',\mathbf{x}_2') d\mathbf{x}_2' dx_1' \\ &= \int_{\mathbb{R}}\int_{\mathbb{R}^2} \left(\int_{\mathbb{R}} u\big((s^2 + |\mathbf{x}_2 - \mathbf{x}_2'|^2)^{1/2}\big) ds \right) f(x_1',\mathbf{x}_2') d\mathbf{x}_2' dx_1' \\ &= \int_{\mathbb{R}^2} \left(\int_{\mathbb{R}} u\big((s^2 + |\mathbf{x}_2 - \mathbf{x}_2'|^2)^{1/2}\big) ds \right) (\mathbf{X} f)(\mathbf{x}_2') d\mathbf{x}_2' \\ &= \int_{\mathbb{R}^2} I_u(|\mathbf{x}_2 - \mathbf{x}_2'|)(\mathbf{X} f)(\mathbf{x}_2') d\mathbf{x}_2' =: \big(I_u(|\cdot|) * \mathbf{X} f\big)(\mathbf{x}_2)\,, \end{aligned} \tag{13}$$

where we defined $I_u(\xi) := \int_{\mathbb{R}} u\big((s^2+\xi^2)^{1/2}\big)ds$.

The relation $\mathbf{X}\mathscr{W}^{3D} = \mathscr{W}^{2D}\mathbf{X}$, identity (13), and the acoustic reciprocal principle Lemma 3.1, imply

$$\begin{aligned}\int_\ell \mathscr{W}^{3D}(U*f)(\mathbf{x},t)dS(\mathbf{x}) &= \big((\mathbf{X}\mathscr{W}^{3D}(U*f)\big)(\mathbf{z},t) = \big(\mathscr{W}^{2D}\mathbf{X}(U*f)\big)(\mathbf{z},t)\\ &= \big(\mathscr{W}^{2D}(I_u(|\cdot|)*\mathbf{X}f)\big)(\mathbf{z},t) = \big(I_u(|\cdot|)*(\mathscr{W}^{2D}\mathbf{X}f)\big)(\mathbf{z},t)\,. \end{aligned} \tag{14}$$

Consequently the left hand sides of (12) and (14) coincide, if

$$w(\xi) = I_u(\xi) = \int_{\mathbb{R}} u\big((s^2+\xi^2)^{1/2}\big)ds = 2\int_\xi^\infty u(\eta)\frac{\eta d\eta}{\sqrt{\eta^2-\xi^2}}\,.$$

This is an Abel integral equation for the function W. Its solution is (see [8, 20])

$$u(\eta) = -\frac{1}{\pi}\int_\eta^\infty \frac{\partial_\xi w(\xi)}{\sqrt{\xi^2-\eta^2}}d\xi\,.$$

This concludes the proof by taking $U = W_{\text{line}}$. □

Next we calculate the point spread function due to finite bandwidth.

Proposition 3.3. *Let $f \in C_c^\infty(\mathbb{R}^3)$ and let $\phi : \mathbb{R} \to \mathbb{R}$ be an even compactly supported function such that $\Phi_{\text{band}}(\mathbf{x}) := -\pi\phi'(|\mathbf{x}|)/(2|\mathbf{x}|)$ is absolutely integrable. Then*

$$\phi *_t \int_\ell (\mathscr{W}^{3D}f)(\mathbf{x},t)d\mathbf{x} = \int_\ell (\mathscr{W}^{3D}\Phi_{\text{band}} * f)(\mathbf{x},t)d\mathbf{x} \tag{15}$$

for any line ℓ outside the support of $\Phi_{\text{band}} * f$.

Proof. Proposition 2.2 states that $\phi *_t (\mathscr{W}^{3D}f) = \mathscr{W}^{3D}(\Phi_{\text{band}} * f)$ outside the support of of $\Phi_{\text{band}} * f$. Integrating this identity over ℓ proves (15). □

Proof of Theorem 2. *According to Propositions 3.2 and 3.3*

$$\phi *_t \int_{\mathbb{R}^3} w\big(\text{dist}(\ell,\mathbf{x})\big)(\mathscr{W}^{3D}f)(\mathbf{x},t)d\mathbf{x} = \phi *_t \int_\ell \mathscr{W}^{3D}(W_{\text{line}} * f)(\mathbf{x},t)d\mathbf{x} = \int_\ell \mathscr{W}^{3D}(\phi *_t W_{\text{line}} * f)(\mathbf{x},t)d\mathbf{x}\,.$$

By taking $\ell = \ell_{\mathbf{z}}$, $\mathbf{z} \in B_R$, and using the support hypothesis on $\phi * w$, this shows $\mathbf{L}_{\phi,w}f = \mathbf{L}(\Phi_{\text{band}} * W_{\text{line}} * f)$. Therefore $\mathbf{L}_{\phi,w}f \in \text{ran}(\mathbf{L})$ and $\mathbf{L}^{-1}\mathbf{L}_{\phi,w}f = \Phi_{\text{band}} * W_{\text{line}} * f$ which concludes the proof.

4 Discussion and Conclusion

In this note we derived analytic expression for the point spread functions in PAT due to the finite detector size and the finite bandwidth of the ultrasound detection system. We showed that the point spread functions due to the finite bandwidth is spatial invariant. The point spread functions due to the detector size is only spatial invariant in the case of approximate line detectors.

The full with half maximum of the point spread function is a typical parameter to measure spatial resolution. Ignoring effects of finite bandwidth, Theorems 1 and 2 show that the lateral resolution of PAT with "approximate point detectors" is $a_{\text{transducer}}|\mathbf{x}|/R$, where $a_{\text{transducer}}$ is the diameter of the ultrasound transducer, and the (uniform) resolution of PAT with "approximate line detectors" is approximately a_{laser}, the width of the detecting laser beam (See Figure 4). Typical values $a_{\text{transducer}} = 2$ cm and $a_{\text{laser}} = 0.1$ cm point out the improved spatial resolution of PAT with integrating line detectors.

5 Acknowledgement

This work has been supported by the Austrian Science Foundation (FWF) within the framework of the NFN "Photoacoustic Imaging in Biology and Medicine", Project S10505-N20. Moreover, the work of M. Haltmeier has been supported by the Technology transfer office of the University Innsbruck (transIT).

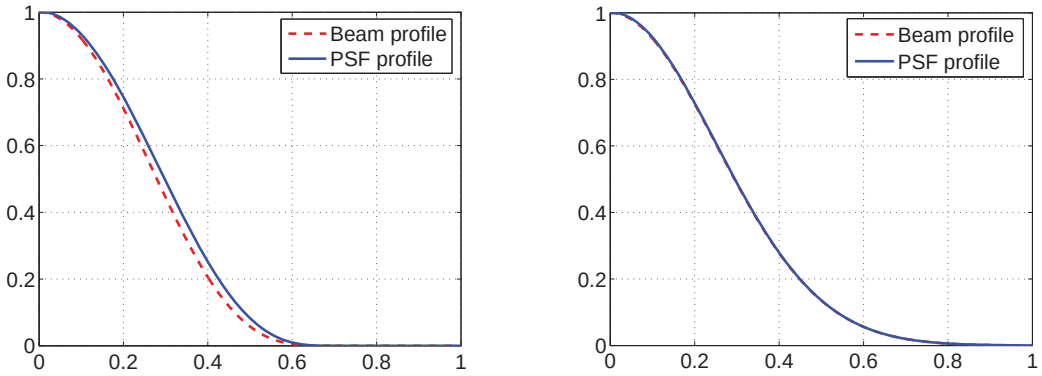

Figure 4: Examples for a beam profile $w(r)$ and profile $-1/\pi \int_r^\infty (\partial_s w)/\sqrt{s^2-r^2}ds$ of the corresponding point spread function $W_{\text{line}}(\mathbf{x})$. One recognizes that the full with half maximum of both functions are similar.

6 References

[1] M. L. Agranovsky and E. T. Quinto. Injectivity sets for the Radon transform over circles and complete systems of radial functions. *J. Funct. Anal.*, 139(2):383–414, 1996.

[2] G. Ambartsoumian and P. Kuchment. On the injectivity of the circular Radon transform. *Inverse Probl.*, 21(2):473–485, 2005.

[3] P. Burgholzer, C. Hofer, G. Paltauf, M. Haltmeier, and O. Scherzer. Thermoacoustic tomography with integrating area and line detectors. *IEEE Trans. Ultrason., Ferroeletr., Freq. Control*, 52(9):1577–1583, 2005.

[4] R. O. Esenaliev, I. V. Larina, K. V. Larin, D. J. Deyo, M. Motamedi, and D. S. Prough. Optoacoustic technique for noninvasive monitoring of blood oxygenation: a feasibility study. *App. Opt.*, 41(22):4722–4731, 2002.

[5] D. Finch, M. Haltmeier, and Rakesh. Inversion of spherical means and the wave equation in even dimensions. *SIAM J. Appl. Math.*, 68(2):392–412, 2007.

[6] D. Finch, S. Patch, and Rakesh. Determining a function from its mean values over a family of spheres. *SIAM J. Math. Anal.*, 35(5):1213–1240, 2004.

[7] D. Finch and Rakesh. Trace identities for solutions of the wave equation with initial data supported in a ball. *Math. Methods Appl. Sci.*, 28:1897–1917, 2005.

[8] R. Gorenflo and S. Vessella. *Abel integral equations*, volume 1461 of *Lecture Notes in Mathematics*. Springer-Verlag, Berlin, 1991. Analysis and applications.

[9] H. Grün, M. Haltmeier, G. Paltauf, and P. Burgholzer. Photoacoustic tomography using a fiber based Fabry–Perot interferometer as an integrating line detector and image reconstruction by model-based time reversal method - article no. 663107. In C. Depeursinge, editor, *Novel Optical Instrumentation for Biomedical Applications III*, volume 6631. SPIE, 2007.

[10] M. Haltmeier and T. Fidler. Mathematical challenges arising in thermoacoustic tomography with line detectors. *arXiv:math/0610155v4*, 2008.

[11] M. Haltmeier, O. Scherzer, P. Burgholzer, R. Nuster, and G. Paltauf. Thermoacoustic tomography & the circular Radon transform: Exact inversion formula. *Math. Models Methods Appl. Sci.*, 17(4):635–655, 2007.

[12] M. Haltmeier, T. Schuster, and O. Scherzer. Filtered backprojection for thermoacoustic computed tomography in spherical geometry. *Math. Methods Appl. Sci.*, 28(16):1919–1937, 2005.

[13] F. John. *Partial Differential Equations*, volume 1 of *Applied Mathematical Sciences*. Springer Verlag, New York, fourth edition, 1982.

[14] R. G. M. Kolkman, E. Hondebrink, W. Steenbergen, and F. F. M. De Mul. In vivo photoacoustic imaging of blood vessels using an extreme-narrow aperture sensor. *IEEE J. Sel. Topics Quantum Electron.*, 9(2):343–346, 2003.

[15] R. A. Kruger, W. L. Kiser, D. R. Reinecke, G. A. Kruger, and K. D. Miller. Thermoacoustic molecular imaging of small animals. *Mol. Imaging*, 2(2):113–123, 2003.

[16] R. A. Kruger, K. D. Miller, H. E. Reynolds, W. L. Kiser, D. R. Reinecke, and G. A. Kruger. Breast cancer in vivo: contrast enhancement with thermoacoustic CT at 434 MHz-feasibility study. *Radiology*, 216(1):279–283, 2000.

[17] L. A. Kunyansky. Explicit inversion formulae for the spherical mean Radon transform. *Inverse Probl.*, 23(1):373–383, 2007.

[18] L. A. Kunyansky. A series solution and a fast algorithm for the inversion of the spherical mean radon transform. *Inverse Probl.*, 23(6):S11–S20, 2007.

[19] S. Manohar, A. Kharine, J. C. G. van Hespen, W. Steenbergen, and T. G. van Leeuwen. The twente photoa-

coustic mammoscope: system overview and performance. *Physics in Medicine and Biology*, 50(11):2543–2557, 2005.

[20] F. Natterer. *The Mathematics of Computerized Tomography*, volume 32 of *Classics in Applied Mathematics*. SIAM, Philadelphia, 2001.

[21] G. Paltauf, R. Nuster, M. Haltmeier, and P. Burgholzer. Experimental evaluation of reconstruction algorithms for limited view photoacoustic tomography with line detectors. *Inverse Probl.*, 23(6):81–94, 2007.

[22] O. Scherzer, M. Grasmair, H. Grossauer, M. Haltmeier, and F. Lenzen. *Variational Methods in Imaging*, volume 167 of *Applied Mathematical Sciences*. Springer, New York, 2008.

[23] X. D. Wang, G. Pang, Y. J. Ku, X. Y. Xie, G. Stoica, and L. V. Wang. Noninvasive laser-induced photoacoustic tomography for structural and functional *in vivo* imaging of the brain. *Nature Biotech.*, 21(7):803–806, 2003.

[24] M. Xu and L. V. Wang. Analytic explanation of spatial resolution related to bandwidth and detector aperture size in thermoacoustic or photoacoustic reconstruction. *Phys. Rev. E*, 67(5):0566051–05660515 (electronic), 2003.

[25] M. Xu and L. V. Wang. Universal back-projection algorithm for photoacoustic computed tomography. *Phys. Rev. E*, 71(1):0167061–0167067 (electronic), 2005.